ACS APPLIED MATERIALS & INTERFACES

Research Article

www.acsami.org

Suppressing Lithium Dendrite Growth with a Single-Component Coating

Haodong Liu, Hongyao Zhou, Byoung-Sun Lee, Xing Xing, Matthew Gonzalez, and Ping Liu*

Department of NanoEngineering, University of California San Diego, La Jolla, California 92093, United States

Supporting Information

ABSTRACT: A single-component coating was formed on lithium (Li) metal in a lithium iodide/organic carbonate [dimethyl carbonate (DMC) and ethylene carbonate (EC)] electrolyte. LiI chemically reacts with DMC to form lithium methyl carbonate (LMC), which precipitates and forms the chemically homogeneous coating layer on the Li surface. This coating layer is shown to enable dendrite-free Li cycling in a symmetric Li||Li cell even at a current density of 3 mA cm^{-2}. Adding EC to DMC modulates the formation of LMC, resulting in a stable coating layer that is essential for long-term Li cycling stability. Furthermore, the coating can enable dendrite-free cycling after being transferred to common $LiPF_6$/carbonate electrolytes, which are compatible with metal oxide cathodes.

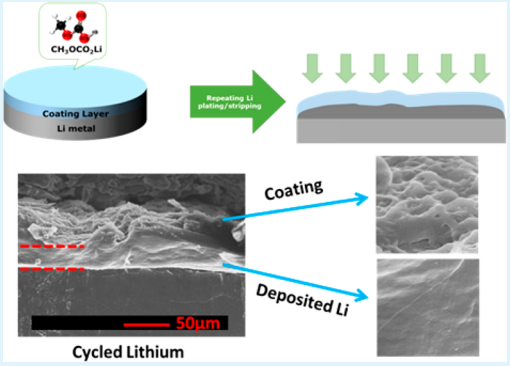

KEYWORDS: *single-component coating, lithium-metal anode, dendrite-free, lithium methyl carbonate, LiI, chemically homogeneous coating*

1. INTRODUCTION

Lithium (Li) metal is being intensively studied as an anode replacement for graphite in Li-ion batteries.[1] A Li-metal anode possesses an extremely high theoretical specific capacity of 3860 mAh g^{-1} and the lowest electrochemical potential (−3.040 V vs SHE) and enables the use of a non-Li-containing cathode, such as sulfur and oxygen.[2,3] However, Li dendrites formed on the electrode surface during repeated charge/discharge can penetrate the separator and create an internal short. In addition, broken dendrites lead to "dead Li" that does not contribute to the cell capacity. Finally, the large surface area of cycled Li also consumes the electrolyte because of their inherent chemical reactivity toward each other.

The reasons for Li dendrite growth, its implications on the battery life, current approaches to overcome it have recently been reviewed.[2−4] In addition to unstable electrodeposition due to concentration gradients in the solution, the chemical reactivity of Li toward battery electrolytes and the subsequent products play an important role in continuous dendrite formation over the lifetime of the battery. Li reacts with the organic solvents and salt anions to form the solid electrolyte interface (SEI), an electronically insulating, but Li-ion-conducting solid layer, which prevents further reduction of the electrolyte.[5−7] The SEI chemical compositions are complex mixtures (ROLi, $ROCO_2Li$, LiF, Li_2O, Li_2CO_3, etc.[6−8]), which are also spatially inhomogeneous (inorganic compounds tend to occupy the interior of the SEI).[2,9] The chemical complexity has resulted in great difficulties in quantifying the compositions and ion-transport mechanisms. More importantly, the chemical heterogeneity of these morphologically homogeneous SEIs intrinsically affects the Li^+ transportation at the Li/electrolyte interface, likely resulting in an inhomogeneous electric-field distribution, which promotes nonuniform Li deposition and stripping.[10] Common SEIs are not mechanically strong enough to accommodate the rapid and large volume changes of the underlying Li during Li plating/stripping. They repeatedly break and reform, consuming newly exposed Li metal and organic electrolyte and generating further morphologically nonuniform SEI layers.[2]

On the basis of these understandings, suppressing Li dendrites can be achieved by mechanical suppression with stiff separators and solid electrolytes or by enhancement of the Li-ion flux uniformity.[4] The latter can be realized with the use of improved electrolytes (such as high Li^+ transference number electrolytes and single-ion conductors) or alternatively by developing an improved SEI, which offers greater chemical and morphological homogeneity.[11] Recent proposals of using high-surface-area 3D hosts for Li metal further demand a high-quality uniform SEI to allow robust Li cycling.[3,12−14] The in situ formation of a more stable SEI has been investigated by tuning the solvents, salts, and additive combinations.[15−22] In addition, ex situ decoration of the Li surface with an artificial SEI layer before assembly into a battery has also been effective.[23−25]

In this work, we make use of the nucleophilic substitution reaction between LiI and dimethyl carbonate to enable the in

Received: June 8, 2017
Accepted: August 22, 2017
Published: August 22, 2017

DOI: 10.1021/acsami.7b08198
ACS Appl. Mater. Interfaces 2017, 9, 30635−30642

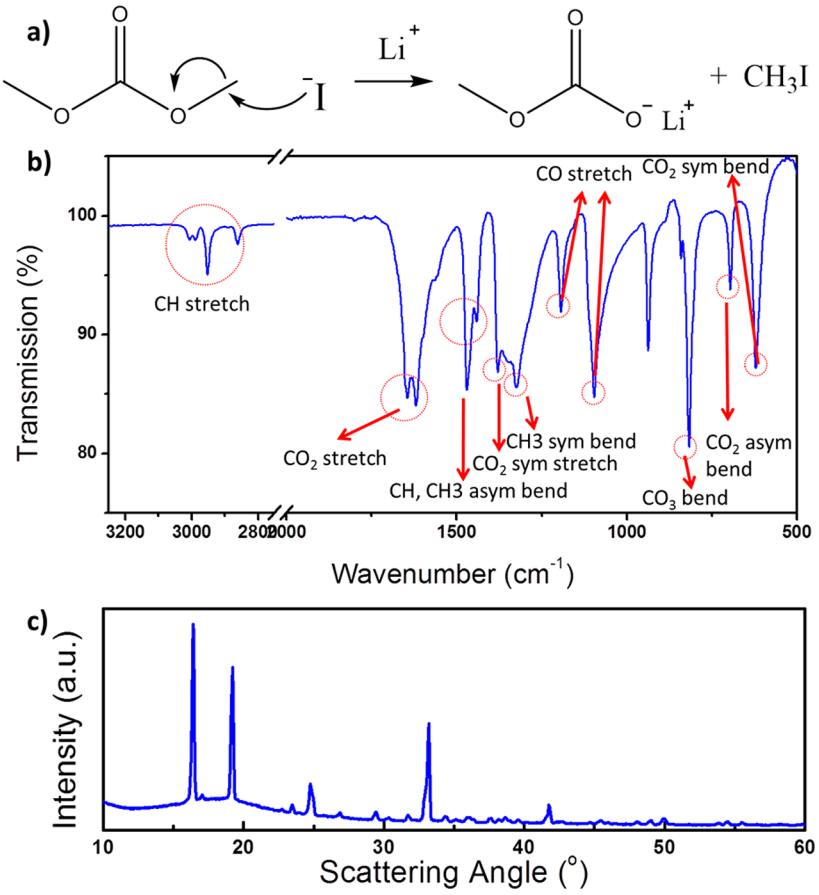

Figure 1. (a) Reaction schematic of DMC and LiI. (b) FTIR spectrum of the precipitate from the DMC and LiI reaction. (c) XRD of the precipitate from the DMC and LiI reaction.

situ formation of a surface layer that is composed of pure lithium methyl carbonate, which we termed a chemically homogeneous coating layer. LiI works as both the Li salt in the electrolyte and a coating formation catalyst. This in situ formation of a coating layer provides a new direction of research for a rationally designed, chemically well-defined coating layer that also enables a dendrite-free Li-metal anode.

2. EXPERIMENTAL METHODS

2.1. Electrolyte Preparation and Electrochemical Test. Battery-grade dimethyl carbonate (DMC), 1,2-dimethoxyethane (DME), ethylene carbonate (EC), and a premixed LP30 electrolyte (1 M $LiPF_6$ in 1:1 EC/DMC volume ratio) were purchased from BASF. LiI beads (ultradry, >99%) were acquired from Alfa Aesar. 2 M LiI−DMC, LiI−EC, LiI−DME, and LiI−EC/DMC electrolytes were prepared by dissolving 2.69 g of LiI in 10 g of DMC, 10 g of EC, 10 g of DME, and 10 g of EC/DMC (1:1 weight ratio) inside an argon-filled glovebox, respectively.

Li||Li symmetric beaker cells were used to study the Li morphology evolution in different electrolytes. Two pieces of Li metal were inserted into the electrolytes inside a glass bottle (herein referred to as a beaker cell); they were electrically connected to copper (Cu) clips. The clips in turn were soldered to Cu wires, which were fed through a rubber stopper that sealed the glass bottle. The distance between two parallel Li plates was fixed at 7 mm. The dimensions of Li immersed in the electrolyte were controlled around 10 mm × 7.5 mm. The current density for Li plating and stripping is calculated based on the measured area considering both the back and front sides of the Li-metal electrodes. All of the beaker cells were tested inside an argon-filled glovebox on a LAND-CT2001A battery test system. The cycled Li anode was recovered by disassembling the beaker cell. All of the Li samples were washed three times with DMC and dried in the glovebox antechamber under vacuum.

2.2. X-ray Diffraction (XRD). The crystal structures of the coating materials were identified by XRD, acquired using a Bruker D8 Advance diffractometer with a Bragg−Brentano $\theta-2\theta$ geometry and a Cu Kα source (λ = 1.54 Å). Samples were sealed inside the glovebox by Kapton tape and scanned from 10° to 60° at a scan rate of 0.05° s^{-1}.

2.3. Fourier Transform Infrared (FTIR) Spectroscopy. FTIR spectroscopy of the coating materials was conducted using a PerkinElmer spectrometer UATR 2 (attenuated-total-reflectance mode and Diamond crystal), scanning from 4000 to 500 cm^{-1} with a resolution of 1 cm^{-1} and averaging over four scans.

2.4. Scanning Electron Microscopy (SEM). The particle morphology and size distribution of the synthesized powders were determined using an FEI/Phillips XL30 ESEM system. All images were collected under an accelerating voltage of 15 kV. Li was adhered to a double-sided carbon tape and placed on a specimen holder. The prepared sample was sealed in a laminate plastic bag inside the glovebox for transfer to the scanning electron microscope. The approximate time of sample exposure to air (from a sealed environment to the SEM stage) was less than 3 s.

3. RESULTS AND DISCUSSION

The goal of the current work is to develop a chemically homogeneous coating layer made of a single, well-defined compound. This approach is expected to offer a highly uniform Li-ion flux through the layer, promoting homogeneous Li plating and stripping. In order to simplify the potential formation reactions, we decided to exclude the possibility of salt anion reductions. Lithium halides are the best choices because the halide anions cannot be further reduced. Among all

DOI: 10.1021/acsami.7b08198
ACS Appl. Mater. Interfaces 2017, 9, 30635−30642

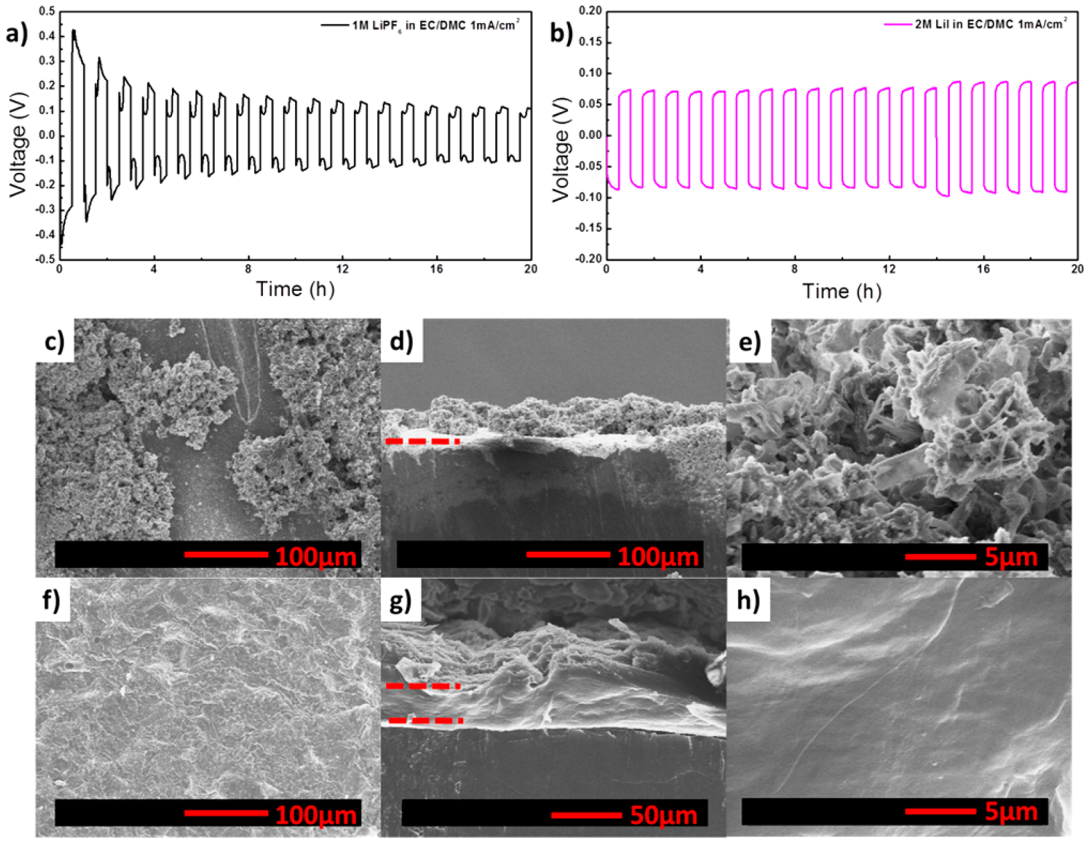

Figure 2. Voltage profiles of the Li||Li cell cycled in (a) 1 M $LiPF_6$ in a EC/DMC (LP30) electrolyte and (b) 2 M LiI−EC/DMC electrolyte over the course of 20 cycles at 1 mA cm^{-2} for 0.5 mAh cm^{-2}: (c) top view and (d and e) cross-sectional view of Li from the LP30 electrolyte cell; (f) top view and (g and h) cross-sectional view of Li from the LiI−EC/DMC electrolyte cell after 20 cycles at 1 mA cm^{-2} for 0.5 mAh cm^{-2}.

of the halides, LiI was chosen for this study for two reasons: LiI has the highest solubility in most organic solvents and is very well-known for its ability to cleave the C−O bond; this may promote the formation of insoluble alkyllithium carbonates, which are often observed in SEI layers.[26]

Figure 1a shows the expected reaction schematic between LiI and DMC. The I^- attacks the methyl group carbon via a nucleophilic substitution reaction and forms CH_3OCO_2Li (LMC) precipitates. Taking advantage of this reaction, we designed a LiI−DMC electrolyte that, in principle, should chemically generate LMC on the Li-metal surface and function as a single-chemical-component surface coating.

A 2 M LiI−DMC electrolyte solution was prepared by dissolving stoichiometric amounts of LiI in DMC. The LiI dissolved rapidly, forming a clear electrolyte solution. The electrolyte was stored inside an argon-filled glovebox for 12 h, where visible white precipitates appeared in the electrolyte after 6 h. These precipitates were filtered and washed three times by DMC and then dried in the glovebox antechamber under vacuum to remove the residual DMC solvent. Figure 1b shows the FTIR spectrum of the precipitates. This FTIR spectrum has also been compared with the LMC data reported in three other studies in Figure S1. The band assignment shows stretching and bending characteristics attributed to the groups of CH_3, CO_2, CH, and CO_3, which are consistent with a LMC structure.[19,27,28] The sharp XRD peaks shown in Figure 1c indicate that LMC possesses a highly crystalline structure.[29]

We employed a simple Li||Li glass beaker cell to detect the Li dendrite formation and investigate the Li morphology evolution over long-term cycling. A Li||Li beaker cell was assembled using the commercial LP30 electrolyte (1 M $LiPF_6$ in 1:1 EC/DMC volume ratio) as a baseline. The cell was cycled at a current density of 1 mA cm^{-2} with a capacity of 0.5 mAh cm^{-2} for 20 cycles. Figure 2a shows the voltage profiles of the Li||Li LP30 (LiL) cell. For each cycle, the decrease in the cell voltage after an initial spike is characteristic of the overpotential associated with the initial electrochemical nucleation of Li.[30] As the cycle number increases, the resistance between the two Li electrodes decreases, as indicated by the decreasing potential gap between Li plating and stripping. This can be attributed to Li dendrite growth and an increase in the electrode surface area. Figure S2a shows optical images of a beaker cell and the Li anode after cycling. After 20 cycles, the originally shiny Li surface turned black. The mossy Li particles suspended in the electrolyte and black surface Li are direct evidence of dendritic Li.[16] The morphology of the cycled Li was examined by SEM in Figure 2c−e, confirming a mossy Li surface that is loose and nonuniform and only partially covers the Li surface.

Figure S3a shows the voltage profile of the Li||Li LiI−DMC (LiD) cell, which was cycled following the same cycling procedure as that for the LiL cell. As a result of the chemical reaction between LiI and DMC, the electrolyte solution is saturated with LMC. The flat Li deposition curve during each cycle suggests no obvious nucleation process during Li plating in this electrolyte.[30] The polarization of plating and stripping increases slowly upon electrochemical cycling, likely as a result of increasing resistance due to the continuous growth of the coating. After 20 cycles, the voltage of the LiD cell is around 320 mV, much higher than 110 mV for the LiL cell. Figure S2b shows optical images of the LiD cell and the Li electrode after

DOI: 10.1021/acsami.7b08198
ACS Appl. Mater. Interfaces 2017, 9, 30635−30642

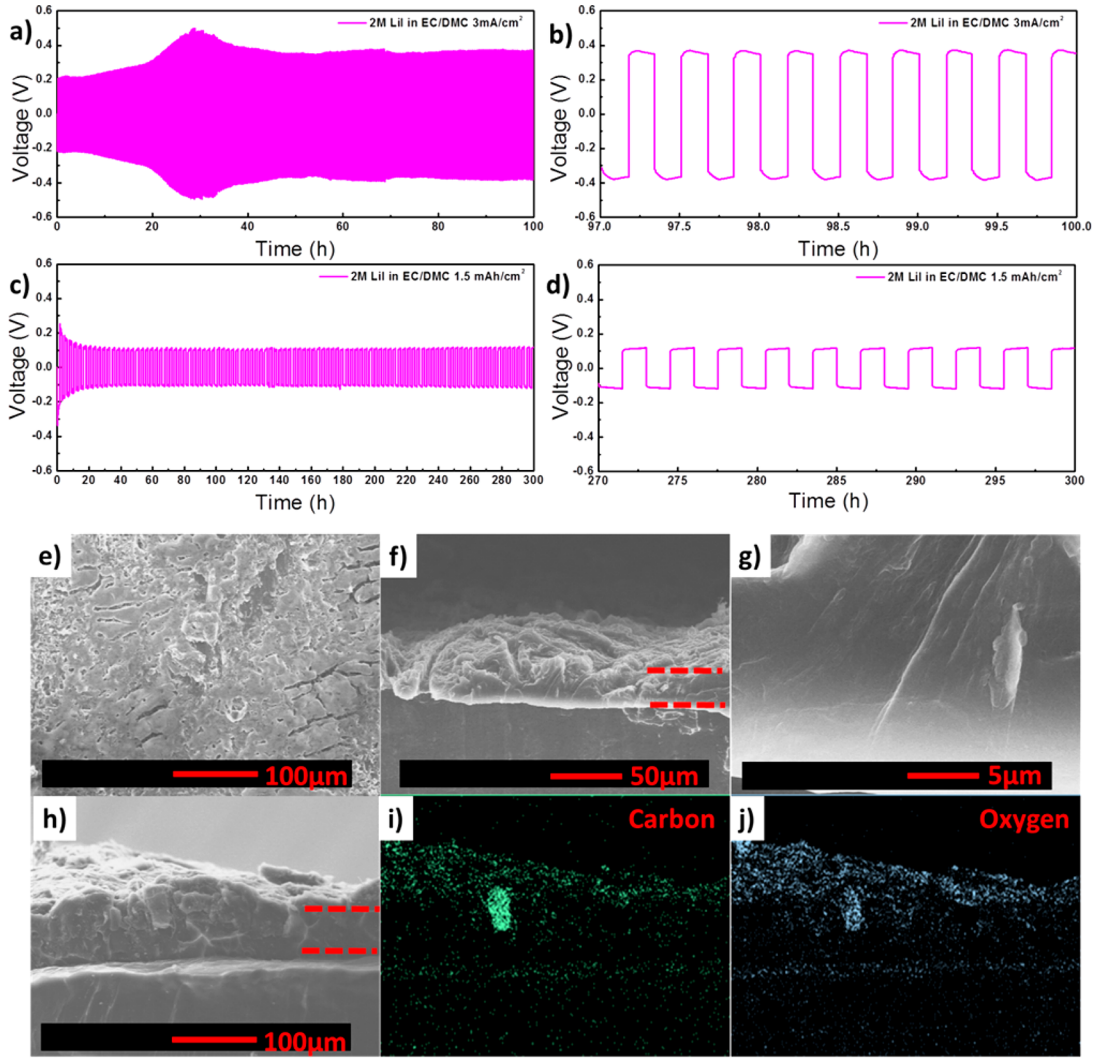

Figure 3. (a) Voltage profiles of the Li||Li cell cycled in a 2 M LiI−EC/DMC electrolyte over the course of 300 cycles at 3 mA cm^{-2} for 0.5 mAh cm^{-2}. (c) Voltage profiles of the Li||Li cell cycled in a 2 M LiI−EC/DMC electrolyte over the course of 100 cycles at 1 mA cm^{-2} for 1.5 mAh cm^{-2}. (b and d) Magnified regions in parts a and c, respectively. SEM images of the cycled Li: (e) top view and (f and g) cross-sectional view of Li from the LiI−EC/DMC electrolyte cell after 300 cycles at 3 mA cm^{-2} for 0.5 mAh cm^{-2}; (h) cross-sectional view of Li from the LiI−EC/DMC electrolyte cell after 100 cycles at 1 mA cm^{-2} for 1.5 mAh cm^{-2}; (i and j) EDS elemental mapping of carbon and oxygen in part h, respectively.

cycling. White precipitates formed on the Li electrode, resulting from the chemical reaction between LiI and DMC, while the electrolyte solution remained free of any floating Li particles or needles. A thick coating was observed on the surface of cycled Li. After washing with DMC, a white dense layer on the Li surface remained. The cycled and washed Li was transferred to a scanning electron microscope to study its morphology. Parts b and c of Figure S3 are top views of the Li electrode at different magnifications, both showing a dense layer fully covering the Li surface. Parts d and e of Figure S3 show cross-sectional views; smooth and dense Li is observed underneath the coating layer with no evidence of dendrites. The SEM images show no dendritic morphology for Li formed in this LiI−DMC electrolyte.

EC is often credited with promoting the formation of high-quality SEI layers.[9] Consequently, we prepared a 2 M LiI−EC electrolyte and fabricated a Li||Li LiI−EC cell. The voltage profile is shown in Figure S4a. The cell voltage stayed around 75 mV over the course of 20 cycles. However, mossy Li was observed inside the beaker. In addition, the surface of the cycled Li showed some black dead Li. There was no effective coating formed on the Li surface in the LiI−EC electrolyte. Likewise, ether-based solvents are also widely reported in studies on dendrite prevention.[2] We then prepared a 2 M LiI−DME electrolyte and fabricated a Li||Li LiI−DME cell. This was cycled following the same conditions as those for the LiL cell. The voltage profile is shown in Figure S5a. The cell suffered from a very high polarization of greater than 800 mV over the course of 20 cycles, implying formation of a highly resistive surface layer. Despite the formation of this surface layer, the optical images of the cycled Li and beaker clearly showed Li dendrite formation.

From these results, it is evident that the beneficial coating is formed only in a LiI−DMC electrolyte and not in LiI−EC or DME. However, this coating appears to continuously grow during electrochemical cycling, resulting in an increase in the cell impedance and polarization. Because the LiI−EC electrolyte resulted in a low overpotential (although it failed to prevent dendrite formation), we next prepared a 2 M LiI−EC/DMC mixed electrolyte with a 1:1 weight ratio of EC and

DOI: 10.1021/acsami.7b08198
ACS Appl. Mater. Interfaces 2017, 9, 30635−30642

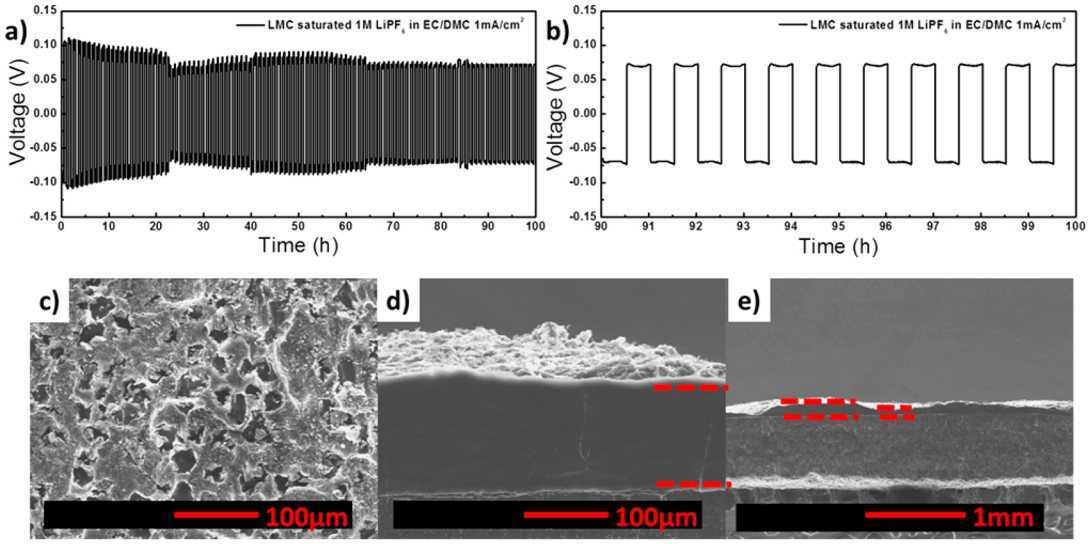

Figure 4. (a) Voltage profiles of the Li||Li cell cycled in LMC-saturated 1 M $LiPF_6$ in a EC/DMC (LP30) electrolyte over the course of 100 cycles at 1 mA cm^{-2} for 0.5 mAh cm^{-2}. (b) Magnified regions in part a. SEM images of cycled Li: (c) top view and (d and e) cross-sectional view of Li from the LMC-saturated LP30 electrolyte cell after 100 cycles at 1 mA cm^{-2} for 0.5 mAh cm^{-2}.

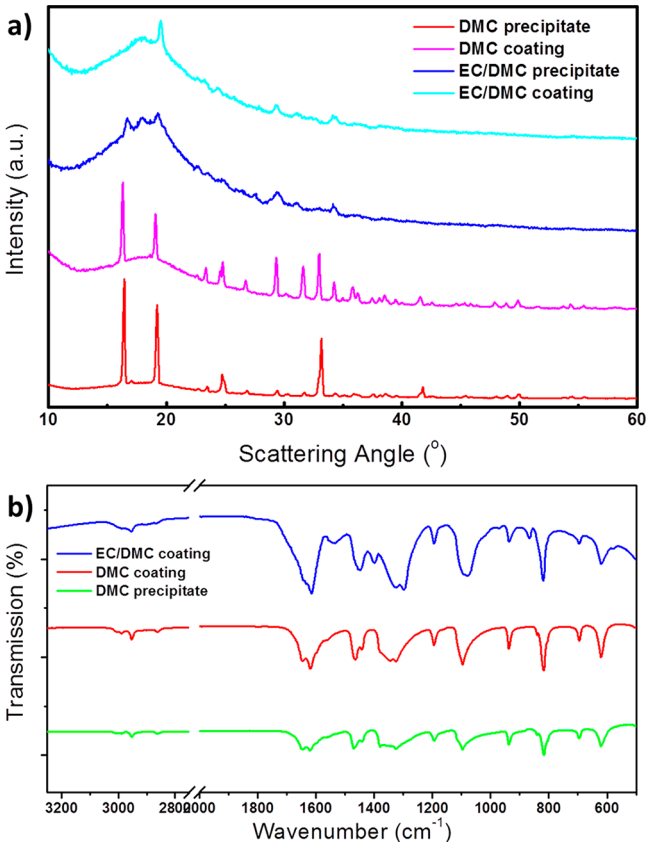

Figure 5. (a) XRD and (b) FTIR spectra of the precipitates and coating from LiI−DMC and LiI−EC/DMC electrolytes.

DMC to benefit from the advantage of both solvents. The Li||Li LiI−EC/DMC (LiED) cell was cycled under conditions identical with those of the LiL cell. Figure 2b shows the voltage profiles over the course of 20 cycles. The voltage profiles do not indicate Li nucleation. Cell polarization was stable at around 85 mV. The electrolyte solution after 20 cycles was clear without any signs of massive Li dendrite formation (Figure S2c), while the cycled Li maintained a thin coating layer. After washing with DMC, the Li electrode still showed metallic reflection. These optical images indicate a dendrite-free morphology. Figure 2f is the top-view SEM image of the dense coating, which continuously covers the Li without evidence of well-defined crystals. Figure 2g is the cross-sectional image of the Li, which shows three distinguishable regions: the underlying uncycled Li substrate, the cycled Li layer, and the coating surface. Figure 2h is the morphology of the deposited Li region, which is dense and smooth. The LiI−EC/DMC electrolyte not only delivered a good electrochemical performance with low polarization but also eliminated the dendritic morphology on the Li.

On the basis of the equation of Sand's time, dendrite formation can be greatly accelerated at high current densities.[2] To test our coating against this, a new LiED cell was prepared and precycled at a current density of 0.67 mA cm^{-2} for 10 cycles over 10 h. A stable coating layer was generated during the precycling. The LiED cell was subsequently cycled at a much higher current density of 3 mA cm^{-2} and a capacity of 0.5 mAh cm^{-2} for 300 cycles. As shown in Figure 3a,b, the polarization at the beginning was around 210 mV, increased as a result of the higher current density. The cell voltage increased because of the SEI growth and then stabilized at around 370 mV. The cycled Li showed a metallic luster (Figure S2d) similar to that of the Li cycled under 1 mA cm^{-2}. Figure 3e is the top-view SEM image of the coating; the layer is dense with some cracks. Parts f and g of Figure 3 display the cross-sectional images of the Li electrode after cycling, which also show a lack of dendritic morphology.

We also examined whether depositing thicker Li would affect its morphology. To test this, another LiED cell was assembled and cycled with a much higher capacity of 1.5 mAh cm^{-2} for 100 times at 1.0 mA cm^{-2}. Figure 3c shows the voltage profiles over the course of 100 cycles. The cross-sectional SEM images shown in Figure 3h suggest that the LiI−EC/DMC electrolyte enables dendrite-free Li morphology with a higher capacity and a longer cycling duration. The intense carbon and oxygen signals gathered from EDS elemental mapping seen in Figure 3i,j from the surface shown in Figure 3h indicate that the layer continuously covers the Li. The quantitative EDS results

DOI: 10.1021/acsami.7b08198
ACS Appl. Mater. Interfaces 2017, 9, 30635−30642

Scheme 1. Schematic Comparison of Li Plating/Stripping between the Traditional SEI and a Chemically Homogeneous Coating

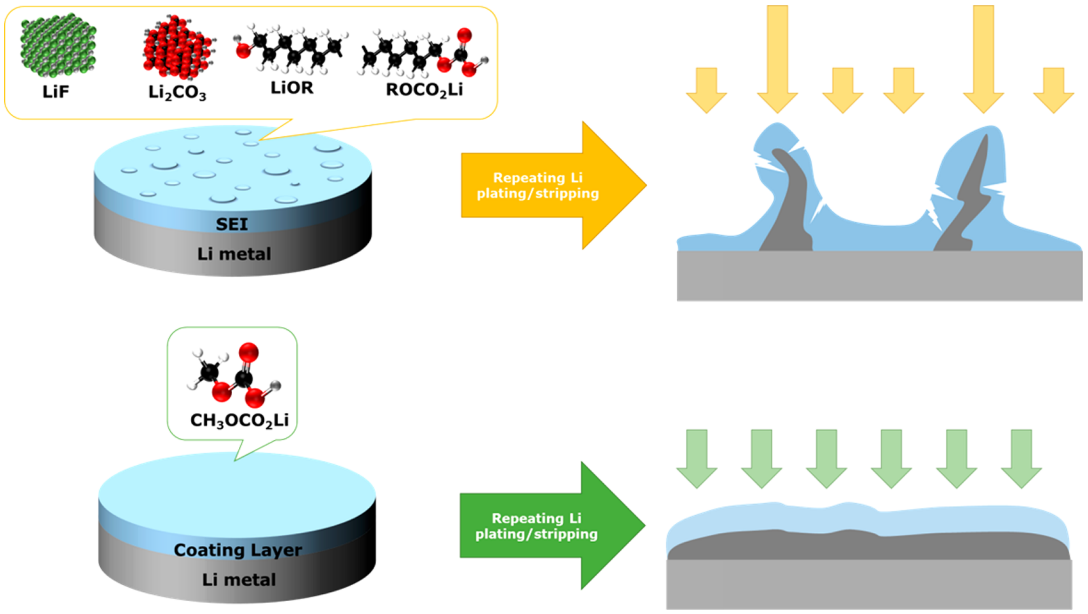

suggest that the O:C ratio is around 1.5, which is consistent with the O:C ratio in LMC. Only a minor iodine signal was detected on the surface region of the coating layer (Figure S7), which might be due to an electrolyte residue during the sample preparation. We thus conclude that the LiI residue is minimal in the coating layer. These results support our suggestion of the formation of a chemically homogeneous coating layer.

Unfortunately, a LiI-based electrolyte is not compatible with common oxide cathode materials that operate at potentials >4 V versus Li/Li^+, higher than the redox potential of I_3^-/I^-.[31−34] In order to investigate the compatibility of this beneficial surface coating layer in other electrolyte systems capable of high potential operation, two Li electrodes were precycled at a current density of 1 mA cm^{-2} for 20 cycles with a total duration of 20 h in a LiD cell. The Li surface was coated with a stable surface layer during the precycling. Subsequently, these Li electrodes were transplanted and assembled in a Li||Li LP30 cell. The LP30 electrolyte was saturated with LMC in case the coating on the Li surface dissolved over time. As shown in Figure 4a,b, this cell was cycled at 1 mA cm^{-2} for 0.5 mAh cm^{-2} for 100 cycles. Figure S2f shows the optical images of the cell and Li electrode after 100 cycles. The electrolyte solution was clear, and the Li electrode still showed luster. Figure 4c shows the top-view SEM image of the coating layer, while parts d and e of Figure 4 display the cross-sectional images of the Li electrode. The deposited Li is still smooth, although the deposition thickness of Li varies in different regions. This experiment proves that the beneficial surface coating prevents Li dendrite formation in electrolytes compatible with oxide cathodes as well.

The novel LiI−EC/DMC electrolyte enabled Li plating and stripping at a very high current density of 3 mA cm^{-2}, maintaining a dendrite-free morphology throughout cycling. The SEM images confirmed that a dense coating layer was formed in the presence of DMC but not in EC alone. In order to further characterize the coating and understand the mechanism, the precipitates and coating were collected from the LiD and LiED cells. These solids were washed three times with DMC and dried under vacuum in the antechamber of the glovebox. We compared our XRD data to those of Xu, who previously modified the Dumas−Peligot synthesis to prepare lithium alkylcarbonates.[27−29] All of the XRD data are plotted in Figure 5a. The precipitate and coating from the LiI−DMC electrolyte were well-crystallized with sharp peaks. All of the major peaks, e.g., 16.4°, 19.2°, and 33.2°, are consistent with the chemically synthesized LMC from Xu's work. The XRD patterns of the precipitate and coating from the LiI−EC/DMC electrolyte were also indexed to LMC. However, their peaks were much broader, which suggested a low degree of coating crystallinity when formed in LiI−EC/DMC. The exact mechanism for EC's function remains an open question. Pure EC does react with LiI to form dilithium ethylene dicarbonate (Figure S8), but its signature is absent in the mixed EC/DMC solvent. In addition, the coating and precipitate formed in LiI−EC appears to be gel-like, which might explain the overall reduction in the crystallinity of the coating in the LiED cell. The FTIR results of the coatings from both Li−DMC and Li−EC/DMC are illustrated in Figure 5b. There are two small additional peaks at around 1400 and 870 cm^{-1}, which can be attributed to residual EC, but the FTIR and XRD results both confirmed that the coating layer is pure LMC.[19,27,28] The reason for a lack of EC/LiI reaction products in an (EC + DMC)/LiI system remains a subject of additional studies.

Scheme 1 compares the different working mechanisms for the traditional SEI and the chemically homogeneous coating layer. The SEI commonly observed on Li surfaces contains compounds from both solvent and salt reduction.[2,9,10,35−37] Under bias, the intrinsic physical properties of these different compounds will likely lead to nonuniform electric fields at the Li and SEI interface. This nonuniformity may, in turn, lead to dendrite formation over the course of long-term cycling. Additionally, nonuniform SEIs are prone to breaking because of the large volume change of the underlying Li. As a consequence, newly deposited Li is exposed to electrolyte and reacts with it to form a new SEI. Our chemically homogeneous coating only contains LMC, which likely provides a uniform distribution of electric fields at the Li and

DOI: 10.1021/acsami.7b08198
ACS Appl. Mater. Interfaces 2017, 9, 30635−30642

SEI interface. The plating or stripping of Li becomes uniform, resulting in a dendrite-free morphology.

4. CONCLUSION

In summary, we propose a new approach to suppressing the Li dendrite through in situ formation of a chemically homogeneous coating layer. This is realized in LiI−DMC and LiI−EC/DMC electrolytes. The surface coating is identified as pure lithium methyl carbonate by XRD and FTIR. Unlike previous reports in using electrolyte additives to suppress dendrites, we made an effort to simplify the cell chemistry to generate a chemically well-defined coating. As a result, the mechanism of dendrite suppression can be unequivocally attributed to this compound. Our coating can sustain cycling at a current density of 3 mA cm^{-2}, which is needed for practical battery applications. The ability of the chemically homogeneous coating to enable dendrite-free Li cycling after being transferred to a different electrolyte opens the possibility of using lithium methyl carbonate as an effective coating on Li surfaces.

■ ASSOCIATED CONTENT

Supporting Information

The Supporting Information is available free of charge on the ACS Publications website at DOI: 10.1021/acsami.7b08198.

Optical images of the beaker and Li after electrochemical cycles from different electrolyte systems, voltage profiles of the Li||Li cell cycled in the LiI−DMC electrolyte and the corresponding SEM images of cycled Li, in the LiI−EC electrolyte and optical images of the beaker and Li, in the LiI−DME electrolyte and optical images of the beaker and Li, and in the LiI−EC/DMC electrolyte at 0.67 mA cm^{-2}, the cross-sectional view of Li from the LiI−EC/DMC electrolyte cell and EDS elemental mapping of carbon, oxygen, and iodine, respectively, and ATIR spectra of precipitates and coating from LiI−EC, LiI−EC/DMC, and LiI−DMC electrolytes (PDF)

■ AUTHOR INFORMATION

Corresponding Author

*E-mail: piliu@eng.ucsd.edu (P.L.).

ORCID

Ping Liu: 0000-0002-1488-1668

Author Contributions

The manuscript was written through contributions of all authors. All authors have given approval to the final version of the manuscript.

Notes

The authors declare no competing financial interest.

■ ACKNOWLEDGMENTS

This work was supported by the Office of Vehicle Technologies of the U.S. Department of Energy through the Advanced Battery Materials Research Program (Battery 500 Consortium) under Contract DE-EE0007764. H.L. acknowledges financial support from the China Scholarship Council under Award 2011631005. We all acknowledge previous discussions with Han Nguyen.

■ REFERENCES

(1) Zheng, J.; Engelhard, M. H.; Mei, D.; Jiao, S.; Polzin, B. J.; Zhang, J.-G.; Xu, W. Electrolyte Additive Enabled Fast Charging and Stable Cycling Lithium Metal Batteries. *Nature Energy* **2017**, *2*, 17012.

(2) Xu, W.; Wang, J. L.; Ding, F.; Chen, X. L.; Nasybulin, E.; Zhang, Y. H.; Zhang, J. G. Lithium Metal Anodes for Rechargeable Batteries. *Energy Environ. Sci.* **2014**, *7* (2), 513−537.

(3) Lin, D.; Liu, Y.; Cui, Y. Reviving the Lithium Metal Anode for High-Energy Batteries. *Nat. Nanotechnol.* **2017**, *12* (3), 194−206.

(4) Tikekar, M. D.; Choudhury, S.; Tu, Z.; Archer, L. A. Design Principles for Electrolytes and Interfaces for Stable Lithium-Metal Batteries. *Nature Energy* **2016**, *1*, 16114.

(5) Peled, E. The Electrochemical-Behavior of Alkali and Alkaline-Earth Metals in Non-Aqueous Battery Systems - the Solid Electrolyte Interphase Model. *J. Electrochem. Soc.* **1979**, *126* (12), 2047−2051.

(6) Aurbach, D.; Zinigrad, E.; Cohen, Y.; Teller, H. A Short Review of Failure Mechanisms of Lithium Metal and Lithiated Graphite Anodes in Liquid Electrolyte Solutions. *Solid State Ionics* **2002**, *148* (3−4), 405−416.

(7) Aurbach, D. Review of Selected Electrode-Solution Interactions Which Determine the Performance of Li and Li Ion Batteries. *J. Power Sources* **2000**, *89* (2), 206−218.

(8) Tan, S.; Ji, Y. J.; Zhang, Z. R.; Yang, Y. Recent Progress in Research on High-Voltage Electrolytes for Lithium-Ion Batteries. *ChemPhysChem* **2014**, *15* (10), 1956−1969.

(9) Xu, K. Electrolytes and Interphases in Li-Ion Batteries and Beyond. *Chem. Rev.* **2014**, *114* (23), 11503−11618.

(10) Cheng, X. B.; Zhang, R.; Zhao, C. Z.; Wei, F.; Zhang, J. G.; Zhang, Q. A Review of Solid Electrolyte Interphases on Lithium Metal Anode. *Adv. Sci.* **2016**, *3* (3), 1500213.

(11) Lu, Y. Y.; Tikekar, M.; Mohanty, R.; Hendrickson, K.; Ma, L.; Archer, L. A. Stable Cycling of Lithium Metal Batteries Using High Transference Number Electrolytes. *Adv. Energy Mater.* **2015**, *5* (9), 1402073.

(12) Yang, C. P.; Yin, Y. X.; Zhang, S. F.; Li, N. W.; Guo, Y. G. Accommodating Lithium into 3D Current Collectors With A Submicron Skeleton Towards Long-Life Lithium Metal Anodes. *Nat. Commun.* **2015**, *6*, 8058.

(13) Zhang, R.; Li, N. W.; Cheng, X. B.; Yin, Y. X.; Zhang, Q.; Guo, Y. G. Advanced Micro/Nanostructures for Lithium Metal Anodes. *Adv. Sci.* **2017**, *4* (3), 1600445.

(14) Ye, H.; Xin, S.; Yin, Y. X.; Li, J. Y.; Guo, Y. G.; Wan, L. J. Stable Li Plating/Stripping Electrochemistry Realized by a Hybrid Li Reservoir in Spherical Carbon Granules with 3D Conducting Skeletons. *J. Am. Chem. Soc.* **2017**, *139* (16), 5916−5922.

(15) Qian, J. F.; Xu, W.; Bhattacharya, P.; Engelhard, M.; Henderson, W. A.; Zhang, Y. H.; Zhang, J. G. Dendrite-free Li Deposition Using Trace-amounts of Water as An Electrolyte Additive. *Nano Energy* **2015**, *15*, 135−144.

(16) Qian, J. F.; Henderson, W. A.; Xu, W.; Bhattacharya, P.; Engelhard, M.; Borodin, O.; Zhang, J. G. High Rate and Stable Cycling of Lithium Metal Anode. *Nat. Commun.* **2015**, *6*, 6362.

(17) Wang, X. M.; Hironaka, T.; Hayashi, E.; Yamada, C.; Naito, H.; Segami, G.; Sakiyama, Y.; Takahashi, Y.; Kibe, K. Electrode Structure Analysis and Surface Characterization for Lithium-ion Cells Simulated Low-Earth-orbit Satellite Operation II: Electrode Surface Characterization. *J. Power Sources* **2007**, *168* (2), 484−492.

(18) Aurbach, D.; Zaban, A.; Schechter, A.; Eineli, Y.; Zinigrad, E.; Markovsky, B. The Study of Electrolyte-Solutions Based on Ethylene and Diethyl Carbonates for Rechargeable Li Batteries 0.1. Li Metal Anodes. *J. Electrochem. Soc.* **1995**, *142* (9), 2873−2882.

(19) Aurbach, D.; Daroux, M. L.; Faguy, P. W.; Yeager, E. Identification of Surface-Films Formed on Lithium in Propylene Carbonate Solutions. *J. Electrochem. Soc.* **1987**, *134* (7), 1611−1620.

(20) Wang, J. H.; Yamada, Y.; Sodeyama, K.; Chiang, C. H.; Tateyama, Y.; Yamada, A. Superconcentrated Electrolytes for a High-voltage Lithium-ion Battery. *Nat. Commun.* **2016**, *7*, 12032.

(21) Ding, F.; Xu, W.; Graff, G. L.; Zhang, J.; Sushko, M. L.; Chen, X. L.; Shao, Y. Y.; Engelhard, M. H.; Nie, Z. M.; Xiao, J.; Liu, X. J.;

DOI: 10.1021/acsami.7b08198
ACS Appl. Mater. Interfaces 2017, 9, 30635−30642

Sushko, P. V.; Liu, J.; Zhang, J. G. Dendrite-Free Lithium Deposition via Self-Healing Electrostatic Shield Mechanism. *J. Am. Chem. Soc.* **2013**, *135* (11), 4450−4456.
(22) Li, N. W.; Yin, Y. X.; Li, J. Y.; Zhang, C. H.; Guo, Y. G. Passivation of Lithium Metal Anode via Hybrid Ionic Liquid Electrolyte toward Stable Li Plating/Stripping. *Adv. Sci.* **2017**, *4* (2), 1600400.
(23) Liu, Y.; Lin, D.; Yuen, P. Y.; Liu, K.; Xie, J.; Dauskardt, R. H.; Cui, Y. An Artificial Solid Electrolyte Interphase with High Li-Ion Conductivity, Mechanical Strength, and Flexibility for Stable Lithium Metal Anodes. *Adv. Mater.* **2017**, *29*, 1605531.
(24) Wang, L.; Wang, Q.; Jia, W.; Chen, S.; Gao, P.; Li, J. Li Metal Coated with Amorphous Li_3PO_4 via Magnetron Sputtering for Stable and Long-cycle Life Lithium Metal Batteries. *J. Power Sources* **2017**, *342*, 175−182.
(25) Li, N. W.; Yin, Y. X.; Yang, C. P.; Guo, Y. G. An Artificial Solid Electrolyte Interphase Layer for Stable Lithium Metal Anodes. *Adv. Mater.* **2016**, *28* (9), 1853−1858.
(26) Charette, A. B.; Barbay, J. K.; He, W. Lithium Iodide. *Encyclopedia of Reagents for Organic Synthesis*; John Wiley & Sons, Ltd., 2001.
(27) Bridel, J. S.; Grugeon, S.; Laruelle, S.; Hassoun, J.; Reale, P.; Scrosati, B.; Tarascon, J. M. Decomposition of Ethylene Carbonate on Electrodeposited Metal Thin Film Anode. *J. Power Sources* **2010**, *195* (7), 2036−2043.
(28) Gireaud, L.; Grugeon, S.; Laruelle, S.; Pilard, S.; Tarascon, J. M. Identification of Li Battery Electrolyte Degradation Products Through Direct Synthesis and Characterization of Alkyl Carbonate Salts. *J. Electrochem. Soc.* **2005**, *152* (5), A850−A857.
(29) Xu, K.; Zhuang, G. R. V.; Allen, J. L.; Lee, U.; Zhang, S. S.; Ross, P. N.; Jow, T. R. Syntheses and Characterization of Lithium Alkyl Mono- and Dicarbonates as Components of Surface Films in Li-Ion Batteries. *J. Phys. Chem. B* **2006**, *110* (15), 7708−7719.
(30) Pei, A.; Zheng, G.; Shi, F.; Li, Y.; Cui, Y. Nanoscale Nucleation and Growth of Electrodeposited Lithium Metal. *Nano Lett.* **2017**, *17* (2), 1132−1139.
(31) Hy, S.; Liu, H. D.; Zhang, M. H.; Qian, D. N.; Hwang, B. J.; Meng, Y. S. Performance and Design Considerations for Lithium Excess Layered Oxide Positive Electrode Materials for Lithium Ion Batteries. *Energy Environ. Sci.* **2016**, *9* (6), 1931−1954.
(32) Liu, H. D.; Chen, Y.; Hy, S.; An, K.; Venkatachalam, S.; Qian, D. N.; Zhang, M. H.; Meng, Y. S. Operando Lithium Dynamics in the Li-Rich Layered Oxide Cathode Material via Neutron Diffraction. *Adv. Energy Mater.* **2016**, *6* (7), 1502143.
(33) Liu, H. D.; Qian, D. N.; Verde, M. G.; Zhang, M. H.; Baggetto, L.; An, K.; Chen, Y.; Carroll, K. J.; Lau, D.; Chi, M. F.; Veith, G. M.; Meng, Y. S. Understanding the Role of NH_4F and Al_2O_3 Surface Co-modification on Lithium-Excess Layered Oxide $Li_{1.2}Ni_{0.2}Mn_{0.6}O_2$. *ACS Appl. Mater. Interfaces* **2015**, *7* (34), 19189−19200.
(34) Trease, N. M.; Seymour, I. D.; Radin, M. D.; Liu, H.; Liu, H.; Hy, S.; Chernova, N.; Parikh, P.; Devaraj, A.; Wiaderek, K. M.; Chupas, P. J.; Chapman, K. W.; Whittingham, M. S.; Meng, Y. S.; Van der Van, A.; Grey, C. P. Identifying the Distribution of Al^{3+} in $LiNi_{0.8}Co_{0.15}Al_{0.05}O_2$. *Chem. Mater.* **2016**, *28* (22), 8170−8180.
(35) Xu, K. Nonaqueous Liquid Electrolytes for Lithium-based Rechargeable Batteries. *Chem. Rev.* **2004**, *104* (10), 4303−4417.
(36) Xiong, D. J.; Petibon, R.; Nie, M.; Ma, L.; Xia, J.; Dahn, J. R. Interactions Between Positive and Negative Electrodes in Li-Ion Cells Operated at High Temperature and High Voltage. *J. Electrochem. Soc.* **2016**, *163* (3), A546−A551.
(37) Ma, L.; Xia, J.; Dahn, J. R. Ternary Electrolyte Additive Mixtures for Li-Ion Cells that Promote Long Lifetime and Less Reactivity with Charged Electrodes at Elevated Temperatures. *J. Electrochem. Soc.* **2015**, *162* (7), A1170−A1174.

DOI: 10.1021/acsami.7b08198
ACS Appl. Mater. Interfaces 2017, 9, 30635−30642